

Scope and Mechanism of the Intermolecular Addition of Aromatic Aldehydes to Olefins Catalyzed by Rh(I) Olefin Complexes

Amy H. Roy, Christian P. Lenges, and Maurice Brookhart*

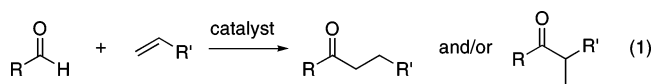
Contribution from the Department of Chemistry, University of North Carolina at Chapel Hill, Chapel Hill, North Carolina 27599-3290

Received September 8, 2006; E-mail: mbrookhart@unc.edu

Abstract: Rhodium (I) bis-olefin complexes $\text{Cp}^*\text{Rh}(\text{VTMS})_2$ and $\text{Cp}^*\text{Rh}(\text{VTMS})_2$ ($\text{Cp}^* = \text{C}_5\text{Me}_5$, $\text{Cp}^\dagger = \text{C}_5\text{Me}_4\text{CF}_3$, VTMS = vinyl trimethylsilane) were found to catalyze the addition of aromatic aldehydes to olefins to form ketones. Use of the more electron-deficient catalyst $\text{Cp}^\dagger\text{Rh}(\text{VTMS})_2$ results in faster reaction rates, better selectivity for linear ketone products from α -olefins, and broader reaction scope. NMR studies of the hydroacylation of vinyltrimethylsilane showed that the starting Rh(I) bis-olefin complexes and the corresponding $\text{Cp}^*/\text{Rh}(\text{CH}_2\text{CH}_2\text{SiMe}_3)(\text{CO})(\text{Ar})$ complexes were catalyst resting states, with an equilibrium established between them prior to turnover. Mechanistic studies suggested that $\text{Cp}^\dagger\text{Rh}(\text{VTMS})_2$ displayed a faster turnover frequency (relative to $\text{Cp}^*\text{Rh}(\text{VTMS})_2$) because of an increase in the rate of reductive elimination, the turnover-limiting step, from the more electron-deficient metal center of $\text{Cp}^\dagger\text{Rh}(\text{VTMS})_2$. Reaction of $\text{Cp}^*/\text{Rh}(\text{CH}_2\text{CH}_2\text{SiMe}_3)(\text{CO})(\text{Ar})$ with PMe_3 yields acyl complexes $\text{Cp}^*/\text{Rh}[\text{C}(\text{O})\text{CH}_2\text{CH}_2\text{SiMe}_3](\text{PMe}_3)(\text{Ar})$; measured first-order rates of reductive elimination of ketone from these Rh(III) complexes established that the Cp^\dagger ligand accelerates this process relative to the Cp^* ligand.

Introduction

During the last two decades, intensive research has been directed toward the transition metal-mediated activation of C–H bonds,^{1–4} including numerous investigations of the C–H bond activation of aldehydes.⁴ Only recently have successful catalytic processes been reported that combine C–H bond activation reactions with C–C bond formation.^{5–10} One of the most developed processes of this kind is the transition metal-catalyzed hydroacylation of olefins. In contrast to established metal-catalyzed X–H addition reactions like the hydrogenation, hydrosilylation, or hydroboration of olefins, the catalytic addition of an aldehyde C–H bond across an olefin to generate a ketone allows the formation of a new carbon–carbon bond in one step with maximum atom economy, while also introducing a versatile functionality, the carbonyl group, to the substrate (eq 1).



Central to the challenge of developing a general and applicable hydroacylation protocol has been controlling regio-

selectivity and eliminating a competing reaction, the transition metal-mediated decarbonylation of aldehydes. Decarbonylation generates the parent alkane and metal carbonyl complexes that are typically inactive or inferior as catalysts for hydroacylation.^{11–17} To circumvent this problem, the groups of James and Bosnich independently reported the intramolecular hydroacylation of 4-pentenal to generate cyclopentanones, with chelation of the substrate believed to facilitate the reaction.^{18–20} However, this intramolecular reaction is specific for the formation of cyclopentanones, and attempts to extend the same catalytic protocol to intermolecular reactions were not successful.

Until recently, strategies utilized for catalytic intermolecular hydroacylation of olefins typically exhibited low productivity and were carried out at high temperatures and/or high pressures to prevent decarbonylation.^{21–23} Alternatively, Jun and co-workers reported the chelation-assisted, Rh-catalyzed intermolecular hydroacylation of olefins in the presence of 2-aminopy-

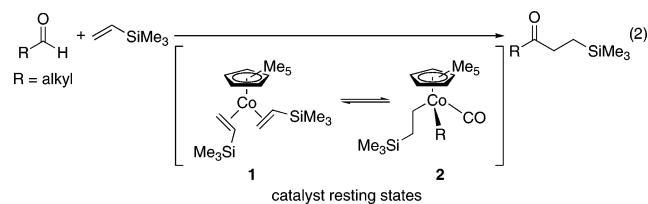
- (1) Bergman, R. G. *Science* **1984**, *223*, 902.
- (2) Jones, W. D. In *Selective Hydrocarbon Activation Principles and Progress*; Davies, J. A., Watson, P. L., Greenberg, A., Liebman, J. F., Eds.; VCH Publishers: New York, 1990; p 113.
- (3) Ryabov, A. D. *Chem. Rev.* **1990**, *90*, 403.
- (4) Shilov, A. E.; Shul'pin, G. B. *Chem. Rev.* **1997**, *97*, 2879–2932.
- (5) Dyker, G. *Angew. Chem., Int. Ed.* **1999**, *38*, 1698–1712.
- (6) Guari, Y.; Sabo-Etienne, S.; Chaudret, B. *Eur. J. Inorg. Chem.* **1999**, 1047–1055.
- (7) Jun, C. H.; Lee, J. H. *Pure Appl. Chem.* **2004**, *76* (3), 577–587.
- (8) Murai, S.; Kakiuchi, F.; Sekine, S.; Tanaka, Y.; Kamatani, A.; Sonoda, M.; Chatani, N. *Pure Appl. Chem.* **1994**, *66*, 1527–1534.

- (9) Ritleng, V.; Sirlin, C.; Pfeffer, M. *Chem. Rev.* **2002**, *102*, 1731–1769.
- (10) Stahl, S. S.; Labinger, J. A.; Bercaw, J. E. *Angew. Chem., Int. Ed.* **1998**, *37*, 2180–2192.
- (11) Abu-Hasanayn, F.; Goldman, M. E.; Goldman, A. S. *J. Am. Chem. Soc.* **1992**, *114*, 2520–2524.
- (12) Milstein, D. *J. Chem. Soc. Chem. Commun.* **1982**, *23*, 1357–1358.
- (13) Milstein, D. *Acc. Chem. Res.* **1984**, *17*, 221–226.
- (14) Ohno, K.; Tsuji, J. *J. Am. Chem. Soc.* **1968**, *90*, 99–107.
- (15) Suggs, J. W. *J. Am. Chem. Soc.* **1978**, *100*, 640–641.
- (16) Tanaka, M.; Sakakura, T. *Pure Appl. Chem.* **1990**, *62*, 1147–1150.
- (17) Tsuji, J.; Ohno, K. *Tetrahedron Lett.* **1967**, *23*, 2173–2176.
- (18) Fairlie, D. P.; Bosnich, B. *Organometallics* **1988**, *7*, 936–945.
- (19) Fairlie, D. P.; Bosnich, B. *Organometallics* **1988**, *7*, 946–954.
- (20) James, B. R.; Young, C. G. *J. Chem. Soc. Chem. Commun.* **1983**, *21*, 1215–1216.

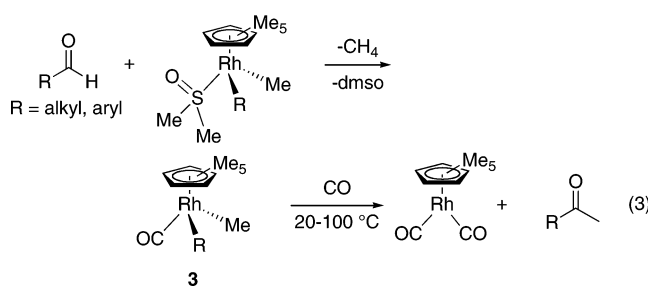
ridine as additive,^{7,24–28} inspired by Suggs' report of the rhodium-catalyzed hydroimination of olefins.²⁹ The proposed mechanism for the chelation-assisted hydroacylation is based on the *in situ* condensation of the aldehyde with the amine additive to generate a chelated imino–rhodium pyridine complex. Subsequent olefin hydroimination and hydrolysis generate the ketone product. This strategy allows olefin coupling to occur while decarbonylation of the aldehyde is avoided. In addition, Jun has extended this chelation-assisted chemistry to include the hydroacylation of alkenes and alkynes with alcohols, as aldehyde precursors, and amines, via imine formation and subsequent hydroiminoacylation.^{30–36} Willis has also utilized a chelation-assisted approach to achieve successful rhodium-catalyzed intermolecular hydroacylation of alkenes or alkynes with aldehydes and imines.^{37–39} Imines, β -thioacetal-substituted esters, and methylsulfanyl-substituted aldehydes were shown to react with acrylate esters, amides, and functionalized alkynes in the presence of Rh(I) catalysts, such as Wilkinson's catalyst and [Rh(dppe)]ClO₄.

We have previously reported the use of labile cobalt(I) bis-olefin complexes as catalysts for the intermolecular anti-Markovnikov addition of aldehydes to vinylsilanes (eq 2).^{40,41} Olefin dissociation from [C₅Me₅Co(C₂H₃SiMe₃)₂], **1**, generated a reactive 16-electron intermediate that could activate an aldehyde C–H bond via oxidative addition. Olefin insertion and reductive elimination from a Co(III) acyl alkyl/aryl intermediate formed the ketone product and regenerated **1** after reaction with olefin. The turnover frequency exhibited a first-order dependence on aldehyde concentration and an inverse first-order dependence on olefin concentration when aromatic aldehydes were employed. The use of alkyl aldehydes resulted in a more complex dependency of the hydroacylation rates on substrate concentrations, suggesting the involvement of a second resting state. This second resting state was observed and identified as a cobalt(III) bis(alkyl) carbonyl complex, **2** (eq 2). The turnover-limiting step for the process was established as the reductive elimination from a cobalt(III) acyl alkyl intermediate formed upon CO

insertion, likely assisted by an η^2 -acyl interaction. A major synthetic limitation of the cobalt system is that simple alkenes such as ethylene, α -olefins, and cyclic olefins are not viable substrates.



The thermolysis of transition metal alkyl or aryl carbonyl complexes to generate ketones stoichiometrically has previously been reported.^{42–45} Most applicable to the work described in this manuscript, Maitlis and co-workers prepared rhodium analogs of **2** via reaction of a rhodium dimethyl precursor with aldehydes.⁴⁶ These complexes generated acetophenone in the presence of excess CO at 20–100 °C (eq 3). The Rh(III)–CO intermediate **3** resembles the observed resting state in the cobalt-catalyzed hydroacylation reactions. However, the barrier for C–C bond formation from a second row metal is expected to be higher than from a first row metal, thus more severe conditions may be required for ketone formation from Rh complexes.



We previously investigated the reactivity of labile rhodium(I) olefin complexes analogous to **1** as catalysts for transfer hydrogenation and the addition of olefins to aromatic ketones.^{47–49} As expected, loss of vinyltrimethylsilane from [C₅Me₅Rh(C₂H₃-SiMe₃)₂] (**4**) generated a reactive 16-electron intermediate that could oxidatively add a variety of C–H bonds. In addition, the bis(propene) analog of **4** has been described as a catalyst for the activation and isomerization of alkyl aldehydes to generate a mixture of isomeric aldehydes.⁵⁰ A rhodium(III) bis(alkyl) carbonyl species was observed as the catalyst resting state for this isomerization process (eq 4), indicating that the C–H activation of aldehydes and subsequent insertion reactions can

- (21) Kondo, T.; Akazome, M.; Tsuji, Y.; Watanabe, Y. *J. Org. Chem.* **1990**, *55*, 1286–1291.
 (22) Marder, T. B.; Roe, D. C.; Milstein, D. *Organometallics* **1988**, *7*, 1451–1453.
 (23) Isnard, P.; Denise, B.; Sneed, R. P. A.; Cognion, J. M.; Durual, P. *J. Organomet. Chem.* **1982**, *240*, 285–288.
 (24) Jun, C. H.; Lee, D. Y.; Lee, H.; Hong, J. B. *Angew. Chem., Int. Ed.* **2000**, *39* (17), 3070–3072.
 (25) Jun, C. H.; Lee, H.; Hong, J. B. *J. Org. Chem.* **1997**, *62*, 1200–1201.
 (26) Jun, C. H.; Moon, C. W.; Lee, D. Y. *Chem.–Eur. J.* **2002**, *8* (11), 2422–2428.
 (27) Jun, C. H.; Hong, J. B.; Lee, D. Y. *Synlett* **1999**, *1*, 1–12.
 (28) Loupy, A.; Chatti, S.; Delamare, S.; Lee, D. Y.; Chung, J. H.; Jun, C. H. *J. Chem. Soc. Perkin Trans. I* **2002**, 1280–1285.
 (29) Suggs, J. W. *J. Am. Chem. Soc.* **1979**, *101*, 489.
 (30) Chang, D. H.; Lee, D. Y.; Hong, B. S.; Choi, J. H.; Jun, C. H. *J. Am. Chem. Soc.* **2004**, *126*, 424–425.
 (31) Jun, C. H.; Chung, K. Y.; Hong, J. B. *Org. Lett.* **2001**, *3* (5), 785–787.
 (32) Jun, C. H.; Huh, C. W.; Na, S. J. *Angew. Chem., Int. Ed.* **1998**, *37* (1/2), 145–147.
 (33) Jun, C. H.; Lee, H.; Hong, J. B.; Kwon, B. I. *Angew. Chem., Int. Ed.* **2002**, *41* (12), 2146–2147.
 (34) Jun, C. H.; Lee, H.; Moon, C. W.; Hong, H. S. *J. Am. Chem. Soc.* **2001**, *123*, 8600–8601.
 (35) Lee, D. Y.; Hong, B. S.; Cho, E. G.; Lee, H.; Jun, C. H. *J. Am. Chem. Soc.* **2003**, *125*, 6372–6373.
 (36) Lee, D. Y.; Moon, C. W.; Jun, C. H. *J. Org. Chem.* **2002**, *67*, 3945–3948.
 (37) Willis, M. C.; McNally, S. J.; Beswick, P. J. *Angew. Chem., Int. Ed.* **2004**, *43*, 340–343.
 (38) Willis, M. C.; Randell-Sly, H. E.; Woodward, R. L.; Currie, G. S. *Org. Lett.* **2005**, *7* (11), 2249–2251.
 (39) Willis, M. C.; Sapmaz, S. *Chem. Commun.* **2001**, 2558–2559.
 (40) Lenges, C. P.; Brookhart, M. *J. Am. Chem. Soc.* **1997**, *119*, 3165–3166.
 (41) Lenges, C. P.; White, P. S.; Brookhart, M. *J. Am. Chem. Soc.* **1998**, *120*, 6965–6979.

- (42) Bianchini, C.; Meli, A.; Peruzzini, M.; Ramirez, J. A.; Vacca, A.; Vizza, F.; Zanobini, F. *Organometallics* **1989**, *8*, 337–345.
 (43) Bianchini, C.; Meli, A.; Peruzzini, M.; Vacca, A.; Zanobini, F. *Organometallics* **1987**, *6*, 2453–2455.
 (44) Saunders, D. R.; Mawby, R. J. *J. Chem. Soc. Dalton Trans.* **1984**, *10*, 2133–2136.
 (45) Schore, N. E.; Ilenda, C. S.; White, M. A.; Bryndza, H. E.; Maturro, M. G.; Bergman, R. G. *J. Am. Chem. Soc.* **1984**, *106*, 7451–7461.
 (46) Sunley, G. J.; Fanizzi, F. P.; Saez, I. M.; Maitlis, P. M. *J. Organomet. Chem.* **1987**, *330* (3), C27.
 (47) Lenges, C. P.; White, P. S.; Brookhart, M. *J. Am. Chem. Soc.* **1999**, *121*, 4385–4396.
 (48) Lenges, C. P.; Brookhart, M. *J. Am. Chem. Soc.* **1999**, *121*, 6616–6623.
 (49) Diaz-Requejo, M. M.; DiSalvo, D.; Brookhart, M. *J. Am. Chem. Soc.* **2003**, *125*, 2038–2039.
 (50) Lenges, C. P.; Brookhart, M. *Angew. Chem., Int. Ed.* **1999**, *38*, 3533–3537.

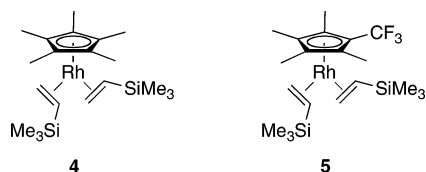
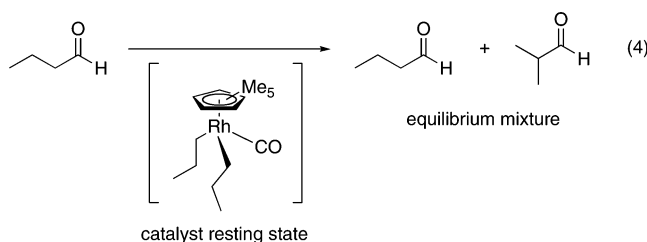


Figure 1. Structures of catalysts **4** and **5**.

occur in this type of system. However, reductive elimination of the hydroacylation product was not observed.



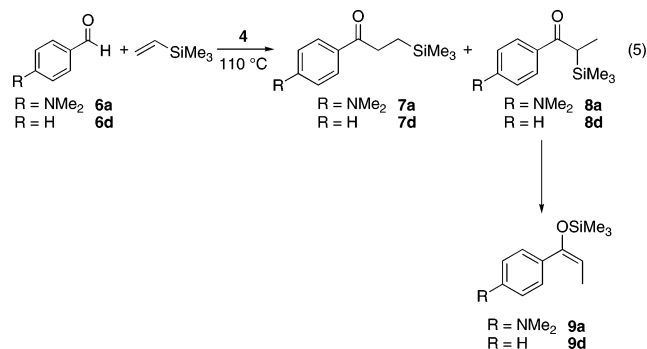
Here we report the use of **4** and a CF₃-substituted derivative of **4** (**5**, Figure 1) as catalysts for the intermolecular hydroacylation of a variety of olefins with aromatic aldehydes. The results reported here combine the prior findings illustrated in eq 3 by Maitlis with the C–H bond activation chemistry observed for systems like **4**. The scope and mechanism for this catalytic process have been investigated, and a more detailed analysis of the turnover-limiting reductive elimination of aryl ketone is described.

Results and Discussion

A. Hydroacylation of Aromatic Aldehydes Using 4. The catalytic hydroacylation of vinyltrimethylsilane with benzaldehyde was studied initially with catalyst **4**. In an experiment followed by ¹H NMR spectroscopy, 5 mol % of **4** was added to a 1:1 mixture of vinyltrimethylsilane and benzaldehyde (**6d**) in *d*₈-toluene. Thermolysis at 110 °C resulted in the slow formation of the hydroacylation product ketone **7d** (eq 5) with a turnover frequency of 2.1 TO/h during the initial stage of catalysis. After 30% conversion, catalyst deactivation generated a blue solution that contained [C₅Me₅Rh(CO)]₂ as the major rhodium species.⁵¹ The formation of this dimer, a product of aldehyde decarbonylation, also explained the appearance of benzene in the reaction mixture.

The use of the more electron-rich substrate *p*-(dimethylamino)benzaldehyde, **6a**, resulted in successful hydroacylation and improved catalyst lifetimes under identical conditions. At 110 °C, an initial turnover frequency of 5 TO/hr was observed to generate ketone. Slow catalyst deactivation resulted in 70% conversion of aldehyde after 20 h. Again, the stoichiometric formation of the parent arene, *N,N*-dimethylaniline, supports decarbonylation as the catalyst deactivation route. Accordingly, the color of the reaction mixture changed during the reaction from the initial orange color of **4** to brown during the catalysis, and then to the intense blue color of the carbonyl-bridged dimer [C₅Me₅Rh(CO)]₂. During the initial phase of catalysis a new, single Rh species was observed, which was assigned as the catalyst resting state. This resting state is discussed in more detail later.

Analysis of the reaction mixture revealed the formation of three different products whose ratios changed as the reaction proceeded. First, the expected anti-Markovnikov addition product ketone (**7a,d**) was observed, analogous to the cobalt-catalyzed process. In addition, a second product based on Markovnikov addition (**8a,d**) was observed in the early stages of the catalytic reaction as indicated by ¹H NMR spectroscopy (quartet at 3.21 ppm, doublet at 1.38 ppm). As the reaction proceeded, a rearrangement of this product occurred to generate the SiMe₃-enol of propiophenone (**9a,d**), as revealed by a decrease in the ketone quartet resonance at 3.21 ppm at the same rate as the formation of a new quartet resonance at 5.05 ppm, assigned to the vinylic hydrogen. After 8 h of reaction, 18% of the Markovnikov ketone was converted to the silyl enol ether **9a**, and 92% conversion to **9a** was observed after 13 h.



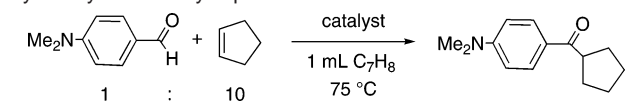
For catalytic reactions on a larger scale, product analysis showed complete conversion of aldehyde to a 2:1 mixture of ketone **7a** and enol **9a** as the only products after extensive reaction time in neat vinyltrimethylsilane. Intermediate **8a** was not detected at this stage.

B. Variation of the Rh Catalyst and Impact on Hydroacylation Activity. Although catalyst **4** showed encouraging activity for the hydroacylation of vinyltrimethylsilane, overall catalytic activity and catalyst lifetime were moderate. While **4** efficiently catalyzed the reaction of electron-donating aldehydes, it was less effective for the reactions of *p*-tolualdehyde and benzaldehyde and was ineffective for reactions of electron-deficient aldehydes. Previous hydroacylation results with cobalt analogs indicated that reductive elimination of ketone could be the rate-limiting step of the reaction.⁴¹ Anticipating that the rate of reductive elimination would increase for a more electron-deficient metal center, catalyst **4** was modified by the substitution of a CF₃ group for a CH₃ group on the Cp* ligand⁵² (Figure 1) in an effort to increase the activity and productivity of the catalyst.

Catalyst **5**, Cp*^{CF₃}Rh(VTMS)₂, was prepared by a similar procedure to that of **4**,⁴⁷ with synthetic details presented in the Experimental Section. Complexes **4** and **5** were compared under identical conditions as catalysts for the reaction between 4-(dimethylamino)benzaldehyde and cyclopentene, with results summarized in Table 1. After 1.5 h at 75 °C, nearly quantitative conversion of aldehyde to ketone was observed for the reaction with catalyst **5**, whereas the reaction with catalyst **4** achieved only 14% conversion of starting material. The substitution of one methyl group in the Cp* ligand by one CF₃ group resulted in a significant increase in catalyst activity for this system.

(51) Nutton, A.; Maitlis, P. M. *J. Organomet. Chem.* **1979**, *166*, C21.

(52) Gassman, P. G.; Mickelson, J. W.; Sowa, J. R., Jr. *Inorg. Synth.* **1997**, *31*, 232–239.

Table 1. Comparison of **4** and **5** as Catalysts for the Hydroacylation of Cyclopentene


entry	catalyst ^a	time (min)	aldehyde:catalyst	% conversion ^b
1	4	90	20:1	14
2	4	180	20:1	24
3	4	360	20:1	50
4	5	90	20:1	98
5	5	180	20:1	>99

^a 5 mol % relative to aldehyde. ^b Conversion monitored by GC.

C. Investigation of the Scope of the Hydroacylation of Olefins Catalyzed by 5. Results for hydroacylation of several olefins catalyzed by the CF₃-substituted catalyst **5** are shown in Table 2. Products were identified by gas chromatography (GC) and NMR spectroscopy after isolation and purification. Isomer mixtures were observed in some cases based on the regiochemistry of the insertion step. The isolated yields reported are the average of two runs.

Reactions were initially performed with a 10:1 ratio of olefin to aldehyde to favor hydroacylation over decarbonylation, but identical yields were obtained when only a 1:1 ratio of olefin to aldehyde was employed (entry 2).⁵³ The addition of both electron-rich and electron-poor benzaldehydes occurred between 75 and 100 °C, but higher catalyst loadings were required and lower yields were obtained for reactions of electron-poor aldehydes. Higher temperatures were required for reactions of unstrained olefins (entries 6 and 9), except when bulky olefins were employed (entry 8). Aryl aldehydes performed well as substrates for these hydroacylation reactions, but the use of alkyl aldehydes resulted in aldehyde isomerization⁵⁰ and no ketone formation.

The reactions catalyzed by **5** were highly regioselective. Reaction between 4-(dimethylamino)benzaldehyde and vinyltrimethylsilane (entry 6) produced only the linear isomer of the ketone product, as opposed to the formation of both the linear and branched products (2:1 ratio) when **4** was used as catalyst. Both the linear and branched products were formed in the reaction of 1-hexene with catalyst **5** (entry 9), but high selectivity for the linear product was observed (22:1 linear:branched product ratio), as compared to the 3:2 linear:branched ratio for the same reaction catalyzed by **4**.

D. Identification of Catalyst Resting States. To identify potential catalyst resting states for this process, the hydroacylation of vinyltrimethylsilane was performed under catalytic conditions and monitored by ¹H NMR spectroscopy. The reaction of 5 mol % **4** with 4-(dimethylamino)benzaldehyde and vinyltrimethylsilane at 110 °C resulted in the formation of a new Cp*⁺-containing species (1.54 ppm, s, 15H) while **4** decreased in intensity. This new complex (**10a**) persisted throughout the initial stages of catalysis, but decreased at later stages of the reaction while the amount of catalyst deactivation products increased. A decrease in catalytic activity paralleled the decrease in the concentration of **10a** in the reaction mixture. The presence of a -SiMe₃ resonance in a 1:1 molar ratio with

the Cp* resonance was observed in the ¹H NMR spectrum of **10a**. In addition, a series of complex resonances was observed in the alkyl region along with a set of aromatic and -NMe₂ resonances that indicate a rhodium-bound *p*-NMe₂-C₆H₄ group. Catalytic conversion of aldehyde was observed efficiently at temperatures above 100 °C. However, the formation of intermediate **10a** was observed at 70 °C with a half-life of formation of ca. 30 min, indicating that the steps to generate intermediate **10a** have a lower barrier than the turnover-limiting step of the reaction. This complex was assigned as Cp*⁺Rh(CH₂CH₂SiMe₃)-(4-NMe₂C₆H₄)(CO) (Scheme 1).⁵⁴ However, the compound was difficult to isolate cleanly for characterization due to the presence of excess aldehyde and because reductive elimination of ketone occurred from this intermediate over time.

Because the rate of reductive elimination of ketone should be slower with a more electron-poor aldehyde, we performed a reaction between **4** and 4-trifluoromethylbenzaldehyde (1:1.1 ratio) in C₆D₆ at room temperature to synthesize a more stable analog of the proposed Rh(III) intermediate. After one week, almost complete conversion of **4** to the Cp*⁺Rh(III) alkyl aryl CO complex (**10e**, Scheme 1) was observed by ¹H NMR spectroscopy with very little ketone formation. After evaporation of the volatile compounds and dissolution of the residue in C₆D₆, the ¹H NMR spectrum of **10e** displayed singlet resonances at 1.35 and 0.04 ppm for the C₅Me₅ and SiMe₃ groups. Highly coupled multiplets characteristic of a -CH₂CH₂- unit (both CH₂ groups are diastereotopic methylene units) were present at 1.86 and 1.77 ppm, (2H, Rh-CHH'), as well as at 1.09 and 1.01 ppm (2H, CHH'-Si). Aromatic resonances between 7.25 and 7.35 ppm (m, 4H) were also observed. The ¹³C NMR spectrum of **10e** also supports the assignment. Resonances for -SiMe₃ (-1.9 ppm, s) and C₅Me₅ (102.2 ppm, d; 8.9 ppm, s) were easily identified. Resonances for the CH₂CH₂ fragment were observed at 18.5 ppm (d) and 26.2 ppm (s). A large quartet assigned to the CF₃ substituent was found at 126.1 ppm (*J*_{CF} = 271 Hz), and the aromatic resonances were located at 124.0 (q, *J*_{CF} = 2.0 Hz), 125.9 (q, *J*_{CF} = 32 Hz), 139.6 (s), and 162.8 ppm (d). The doublet resonance at 162.8 ppm suggested the formation of an Rh-aryl bond and was confirmed by the observation of a doublet resonance at 194.0 ppm, assigned to the Rh-CO. No resonances for the branched isomer **10'e**, Cp*⁺-Rh(CH(CH₃)SiMe₃)(C₆H₄CF₃)(CO), could be detected (<ca. 5%, the detection limit). The formation of similar intermediates was also observed for reactions with other aldehydes.

The corresponding proposed Rh(III) resting state for hydroacylations catalyzed by **5** was synthesized via the reaction of **5** with 4-(dimethylamino)benzaldehyde at 50 °C (Scheme 1). Again, species **11a** easily underwent reductive elimination of ketone, preventing clean isolation of the desired Rh(III) intermediate. The ¹H NMR spectrum of **11a** generated *in situ* revealed singlet resonances at 0.037 and 2.58 ppm for the SiMe₃ and NMe₂ functionalities. Four singlets appeared at 1.21, 1.28, 1.68, and 1.78 ppm for the inequivalent cyclopentadienyl methyl groups, whereas 2 broad multiplets at 1.15 and 2.15 ppm were assigned to the CH₂ groups of the -CH₂CH₂SiMe₃ unit bound

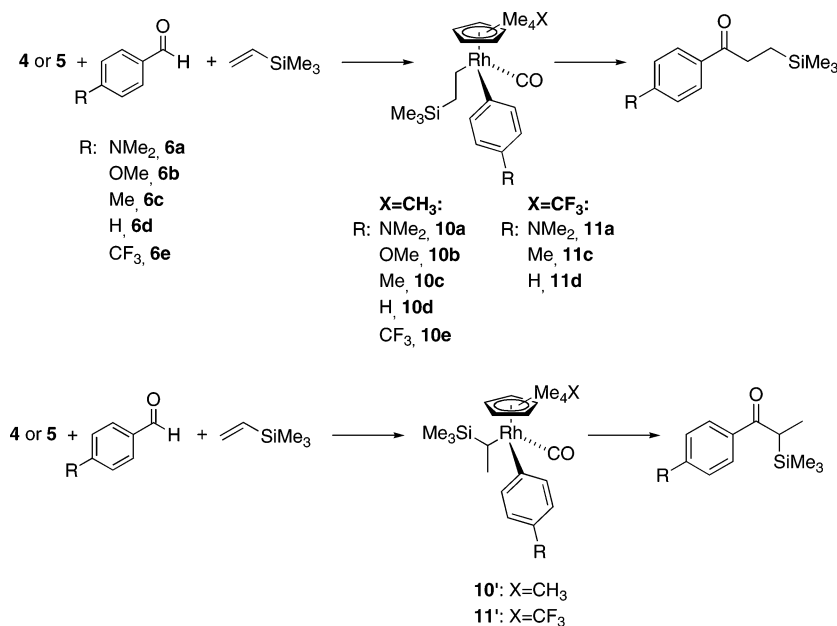
(53) Although our standard conditions for comparison of substrates involves the use of a 10:1 ratio of olefin:aldehyde, the single successful run employing a 1:1 ratio of olefin:aldehyde (entry 2, Table 2) is likely to be generally applicable to all olefins.

(54) Comparison of the signals of **10a** with the analogous species, **10e**, generated from *p*-CF₃C₆H₄CHO (see below) clearly establish **10a** as Cp*⁺(CH₂CH₂-SiMe₃)(C₆H₄NMe₂)(CO). Traces of a second complex are evident (doublet at 7.32 ppm, 2 overlapping doublets (1 corresponding to this second complex, 1 to the silyl enol ether product) at 6.61 ppm, a singlet at 2.63 ppm for NMe₂, and a singlet at 1.54 ppm for Cp*), which may be due to the branched isomer **10'a**, but this assignment is tentative.

Table 2. Hydroacylation of Olefins Catalyzed by **5**

Entry	R	Olefin	Product	Conditions	Time (h)	% Yield ^b
1	NMe ₂			5 mol% Rh, 75 °C	1.5	91
2 ^a	NMe ₂			5 mol% Rh, 75 °C	3	92
3	OMe			7 mol% Rh, 75 °C	2	94
4	Me			7 mol% Rh, 75 °C	6	81
5	CF ₃			11 mol% Rh, 100 °C	48	25 ^c
6	NMe ₂			5 mol% Rh, 100 °C	12	85 (linear isomer only)
7	NMe ₂			5 mol% Rh, 75 °C	3	96
8	NMe ₂			5 mol% Rh, 75 °C	6	97
9	NMe ₂			5 mol% Rh, 100 °C	6	86 (linear : branched = 22 : 1)

^a Olefin:aldehyde = 1:1. ^b Isolated yields are the average of 2 runs, unless otherwise noted. ^c GC yield.

Scheme 1

to rhodium. The aromatic protons exhibited doublet resonances at 6.66 and 7.13 ppm.

A series of resting state analogs for different aromatic aldehydes was generated *in situ* and characterized by IR spectroscopy. The ν_{CO} values for these resting state species are shown in Figure 2. The para substituent of the Rh-bound phenyl group appears not to strongly influence the CO stretch, as suggested by the similar ν_{CO} values for both electron-donating and electron-withdrawing substituents. However, the trend shows a small increase in CO bond strength as the phenyl substituent becomes more electron-deficient. As discussed earlier, longer lifetimes and higher turnover numbers are typically achieved with a more electron-rich substrate. The

substitution of an electron-withdrawing group on the Cp* ligand shows a more pronounced effect on the CO stretching frequency, as seen by the difference in frequency between **10d** and **11d** (Figure 2).

The reaction between 4-(dimethylamino)benzaldehyde and vinyltrimethylsilane (1:2 ratio) catalyzed by **5** (15 mol % relative to aldehyde) was performed at 50 °C and monitored by ¹H NMR spectroscopy to identify the catalyst resting state(s) under conditions where turnover is occurring, but at a sufficiently slow rate that intermediates can be easily detected. Surprisingly, only a trace amount of the Rh(III) species **11a** is present in solution after 6 h, even though hydroacylation product is slowly being formed. The major Rh species present is the starting Rh(I) bis-

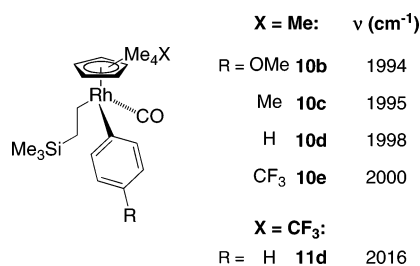


Figure 2. CO stretching frequencies for Rh(III) resting states **10** and **11**.

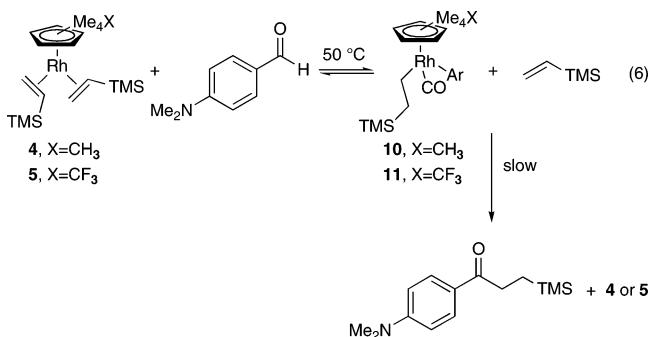
Table 3. Dependence of Rh(I):Rh(III) Resting States on Aldehyde:Olefin Ratio^a

X	aldehyde:olefin	Rh(I):Rh(III)
CF ₃		5:11
	1:2	17:1
	5:1	2:1
CH ₃		4:10
	1:2	4.5:1
	5:1	0.8:1

^a Typical reaction conditions: 140 mM aldehyde, 21 mM **4** or **5**, 0.5 mL C₆D₆, 50 °C in a J Young tube. Reactions were monitored by ¹H NMR spectroscopy.

olefin complex **5**. The ratio of the Rh(I):Rh(III) species was studied as a function of the initial aldehyde:olefin ratio. This data is summarized in Table 3 for both **5** and the less-electrophilic complex **4**. For each complex, the ratio of Rh(III):Rh(I) increases with an increase of the aldehyde:olefin ratio. A comparison of the two systems under identical conditions shows that the Rh(I):Rh(III) ratio is greater by a factor of 6–8 for the CF₃-substituted complex **5**. This outcome might be expected because the stronger electron-withdrawing Cp* ligand should favor Rh(I) over Rh(III) to a greater extent than the Cp* ligand. Once product begins to appear, the ratios of the Rh(I):Rh(III) species remain unchanged.

These experiments strongly suggest that the bis-olefin complexes **4** and **5** are in equilibrium with the alkyl aryl carbonyl Rh(III) species prior to product formation, as shown in eq 6. The equilibration of these two rhodium species is further examined and verified in the next section.



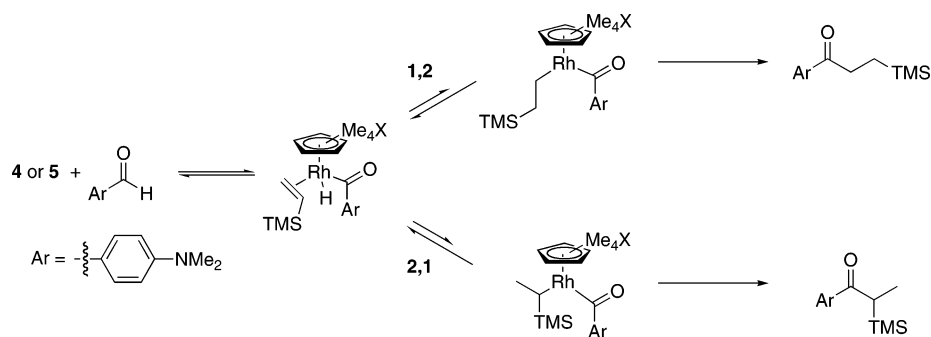
E. Investigation of Reversibility in the Hydroacylation Mechanism. Resting states **10** and **11** are generated by a sequence of reactions including C–H activation of the aldehyde, olefin insertion into the Rh–H bond, and CO deinsertion from the resulting rhodium acyl complex. Reactions between vinyltrimethylsilane and 4-(dimethylamino)benzaldehyde-*d*₁ were performed with both **4** and **5** to gain mechanistic information about these three early steps of the catalytic cycle.

In an NMR tube, complex **4** was dissolved in C₆D₆ and combined with 20 equiv of 4-(dimethylamino)benzaldehyde-*d*₁ and 20 equiv of vinyltrimethylsilane. The reaction mixture was heated to 80 °C and followed by ¹H NMR spectroscopy. As hydroacylation was observed slowly under these conditions, a ¹H aldehyde signal grew into the ¹H NMR spectrum to about 20% of the normalized aldehyde resonance in the aryl region. This observation suggests reversible aldehyde activation and olefin insertion prior to slow, turnover-limiting reductive elimination. Significantly, the –CH₂– resonances of the generated ketone, H₂NC₆H₄C(O)CH₂CH₂SiMe₃, showed approximately equal integral areas and, as expected, a reduction in integration due to deuterium incorporation. For example, after 3 days under these conditions only 60% intensity was observed for each –CH₂– group, which indicates a reversible H/D exchange prior to ketone formation. The equal incorporation of deuterium into both sites of the linear –CH₂–CH₂– chain suggests that reversible 1,2 and 2,1 insertion occurs to scramble D equally into the α and β sites prior to ketone formation (see Scheme 2).

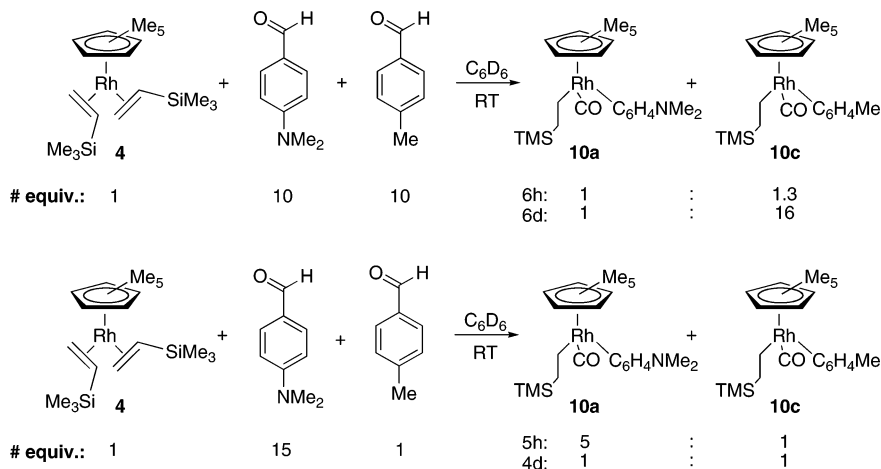
A similar reaction was performed with complex **5**. In an NMR tube, 20 equiv of 4-(dimethylamino)benzaldehyde-*d*₁ and 20 equiv of vinyltrimethylsilane were added to a solution of **5** in C₆D₆. The solution was heated at 50 °C and monitored by ¹H NMR spectroscopy. Again, a ¹H aldehyde signal grew into the ¹H NMR spectrum to about 30% of the normalized aldehyde resonance, in agreement with reversible oxidative addition and insertion observed for the reaction of **4**. However, unlike the reaction with **4**, the –CH₂– resonances of the generated ketone did not integrate equally. Rather, the CH₂ group α to the –SiMe₃ group decreased in intensity more than the CH₂ β to the –SiMe₃ group. For example, as ketone formed after 4 days at 50 °C, only 61% intensity was observed for the CH₂ group α to –SiMe₃ whereas 91% intensity was observed for the CH₂ group β to –SiMe₃. The lack of significant D incorporation into the β site and the high selectivity for formation of the linear ketone in the case of **5** (>99:1 linear:branched) indicates that, in contrast to the catalytic reaction with **4** described above, little 2,1 insertion occurs prior to formation of linear ketone (see Scheme 2).

Aldehyde exchange experiments were also performed to gain insight about reversibility of the CO deinsertion step. Ten equivalents of both 4-(dimethylamino)benzaldehyde (**6a**) and *p*-tolualdehyde (**6c**) were added to 1 equiv of **4** in C₆D₆. The reaction was performed at room temperature and monitored by ¹H NMR spectroscopy. The formation of the corresponding Cp*Rh(aryl)(CH₂CH₂SiMe₃)(CO) complexes (**10a,c**) in a nearly 1:1 ratio was observed after 6 h, indicating no kinetic preference for the formation of one product over the other (Scheme 3). However, after 6 days, the tolualdehyde complex **10c** was favored over the corresponding (dimethylamino)benzaldehyde complex (**10a**) by a ratio of 16:1, demonstrating the establishment of an equilibrium between **4** and the Rh(III) intermediates **10a** and **10c** over time. In a second confirming experiment, a 1:15:1 ratio of **4**:**6a**:**6c** was similarly monitored at 50 °C by ¹H NMR spectroscopy. Under these conditions, formation of the Rh(III) (dimethylamino)benzaldehyde complex **10a** was favored at early reaction times due to the large excess of 4-(dimethylamino)benzaldehyde in solution. However, after 4 days, a 1:1 ratio of the Cp*Rh(III) complexes was established, supporting

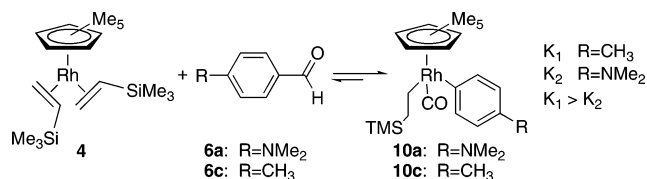
Scheme 2



Scheme 3



Scheme 4



the reversibility of the CO deinsertion step, along with the oxidative addition and olefin insertion steps.

That **10c** is favored over **10a** in the equilibrium described in Scheme 3 implies that K_1 is greater than K_2 in the equilibria illustrated in Scheme 4.

The results in Scheme 4 are easily rationalized by considering substituent effects on both the free aldehydes and rhodium aryl species, **10a/10c**. Aldehyde **6a** is strongly stabilized through a resonance interaction of the dimethylamino group with the aldehyde functionality whereas no such stabilization is present in tolualdehyde. In the rhodium aryl complex **10a**, no equivalent resonance stabilization is possible, thus the fact that $K_2 < K_1$ can be largely attributed to strong resonance stabilization of **6a**. The observation that there is no kinetic preference for formation of **10a** vs **10c** suggests that, as in the ground state,

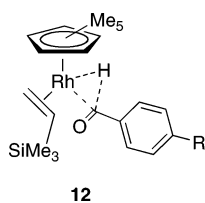
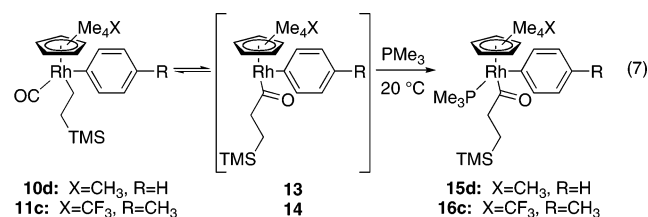


Figure 3. Transition state structure for C–H bond activation step.

there is a substantial resonance interaction of the Me₂N group with the carbonyl functionality in the transition state for formation of complexes **10a,c** from **4**. In other words, para-substituent effects on stabilities are similar for the aldehydes **6a,c** and for the transition states for formation of **10a,c**. A transition state involving C–H addition to the Rh center (**12**, Figure 3) is consistent with this view.

F. Reactivity of Resting State 10/11 with PMe₃. We next investigated the reactivity of intermediates of type **10/11** with a trapping ligand to learn more about the reductive elimination of ketone. Complex **10d** was generated *in situ* by the reaction of benzaldehyde with **4** (ratio 1:1.1) in toluene-*d*₈. Excess benzaldehyde was removed under vacuum and the isolated complex **10d** used without further purification. Ten equivalents of PMe₃ were added to a solution of **10d** in C₆D₆ at room temperature, and the reaction was followed by NMR spectroscopy. Reversible CO insertion (see kinetic studies below) generates an acyl aryl intermediate **13** that is rapidly trapped by PMe₃ to readily form the acyl-aryl complex **15d** at room temperature (eq 7).



Orange crystals of **15d** were obtained from the reaction mixture after cooling to -30 °C (Figure 4). The regiochemistry

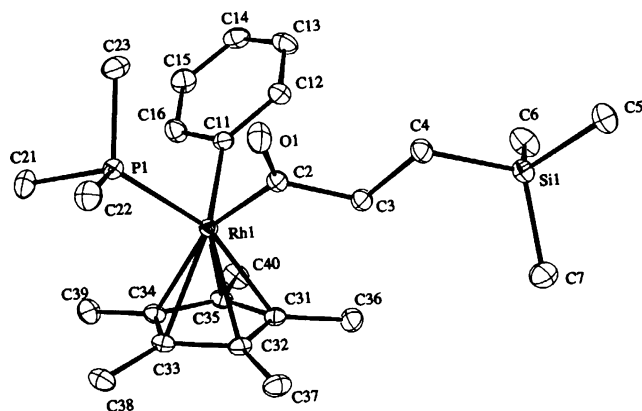


Figure 4. ORTEP diagram of complex **15d**; ellipsoids are drawn with 50% probability. Selected bond distances (Å) and angles (deg) are provided in Table 4.

Table 4. Selected Bond Distances and Angles for **15d**

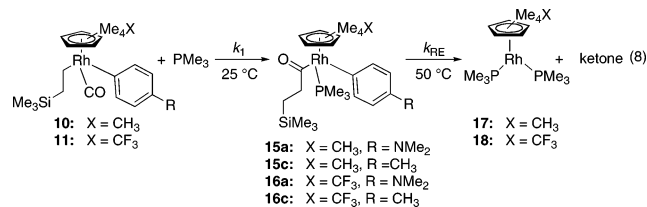
bond lengths (Å)		bond angles (deg)	
Rh–P	2.2534(3)	P–Rh–C2	86.26(4)
Rh–C2	2.0183(13)	P–Rh–C11	88.21
Rh–C11	2.0636(12)	C2–Rh–C11	88.07(5)
O–C2	1.2203(16)	Rh–C2–O	126.62(10)
C4–Si	1.8710(14)	Rh–C2–C3	116.14(9)
		O–C2–C3	117.23(11)
		Si–C4–C3	111.96(9)
		Rh–C11–C12	126.84(10)
		Rh–C11–C16	118.01(10)

of the proposed structure for **15d** was confirmed by X-ray crystallography. Insertion of CO into the rhodium-alkyl bond, not the rhodium-aryl bond, is clearly observed in the crystal structure. Selected bond distances and angles for **15d** are provided in Table 4. Key ^1H NMR data for **15d** include a doublet resonance at 1.03 ppm for the rhodium-bound PMe_3 ligand, and four highly coupled multiplets at 1.18, 1.31, 2.69, and 3.43 ppm corresponding to the two sets of diastereomeric methylene protons of $\text{C}(\text{O})\text{CH}_2\text{CH}_2\text{SiMe}_3$. The multiplets at 2.69 and 3.43 ppm are shifted significantly downfield compared to the $\text{Cp}^*\text{Rh}(\text{CH}_2\text{CH}_2\text{SiMe}_3)(\text{Ph})(\text{CO})$ precursor **10d** due to the insertion of CO into the rhodium alkyl bond. The ^{13}C NMR spectrum displays a doublet for the rhodium-bound PMe_3 ligand at 14.85 ppm, and singlets at 13.47 and 51.75 ppm for the CH_2 groups of the acyl ligand. The resonance at 51.75 ppm is again shifted downfield compared to **10d** due to the insertion of CO into the rhodium alkyl bond.

The analogous intermediate with the more electron-deficient catalyst **5** was also prepared. Complex **11c** was generated *in situ* by the reaction of 10 equiv of *p*-tolualdehyde with **5** at room temperature in C_6D_6 . Excess aldehyde was needed to increase the rate of oxidative addition at room temperature, but was then not able to be separated from **11c**. Five equivalents of PMe_3 were added to the solution of **11c**, and the formation of PMe_3 -trapped **16c** at room temperature was monitored by ^1H and ^{31}P NMR spectroscopy (eq 7). ^{31}P NMR spectroscopy showed the appearance of a doublet at 14.0 ppm ($J = 184.5$ Hz), indicating a new rhodium-bound phosphine, as the peak corresponding to free PMe_3 decreased in intensity. The disappearance of signals corresponding to the four cyclopentadienyl methyl groups was observed by ^1H NMR spectroscopy, along with the appearance of new cyclopentadienyl methyl signals at 1.92 (br d, 3H), 1.79 (br d, 3H), and 1.53 ppm (d, $J = 1.6$ Hz,

6H). The signals corresponding to the CH_2 groups of **11c** disappeared and were replaced by highly coupled resonances at 3.35 (1H), 2.50 (1H), and 1.20 (1H) ppm, with the fourth resonance hidden underneath another peak. The appearance of a new doublet at 1.05 ppm (d, $J = 9.6$ Hz) indicates a rhodium-bound PMe_3 ligand.

Rate constants for CO insertion and subsequent trapping of the resulting intermediate by PMe_3 were measured by ^1H NMR spectroscopy at 25 °C. Complex **11c** was generated *in situ* from the reaction between **5** (0.035 M) and *p*-tolualdehyde (0.42 M) in C_6D_6 , with 1,3,5-trimethoxybenzene present as internal standard. Once complete conversion of **5** to **11c** was observed by ^1H NMR spectroscopy, 5 or 10 equiv of PMe_3 (0.18 or 0.36 M) were added to the NMR tube, and the reaction to form **16c** was monitored by ^1H NMR spectroscopy at 25 °C. Clean first-order kinetics were observed with measured rate constants of $0.50 \times 10^{-4} \text{ s}^{-1}$ and $1.1 \times 10^{-4} \text{ s}^{-1}$ for reactions with 5 and 10 equiv PMe_3 , respectively. The observed first-order dependence of rate on $[\text{PMe}_3]$ show that CO insertion is fast and reversible, followed by rate-determining trapping by PMe_3 . Identical reactions were performed with **10c**, generated *in situ* by reaction between **4** and *p*-tolualdehyde. Rate constants of $0.83 \times 10^{-4} \text{ s}^{-1}$ and $1.5 \times 10^{-4} \text{ s}^{-1}$ were measured for the reaction to form **15c** with 5 and 10 equiv of PMe_3 , respectively.

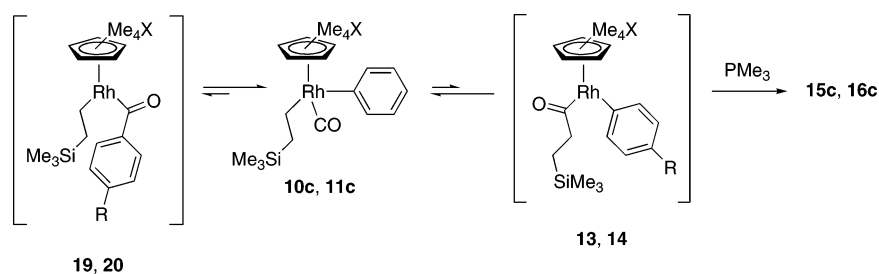


The formation of **15c** and **16c** must involve rapid and reversible formation of acyl aryl complexes **13** and **14** followed by rate-determining trapping by PMe_3 . In general, CO insertions into Rh–C(sp³) bonds are slow compared to insertion into Rh–C(sp²) bonds⁵⁵ and thus it seems likely that carbonyl complexes **10c**, **11c** are in rapid equilibrium with both the aryoyl alkyl species **19**, **20** and the acyl aryl species **13**, **14**. The latter species are then selectively trapped by PMe_3 to yield **15c**, **16c** as shown in Scheme 5. Supporting the contention that **10c**, **11c** are in equilibrium with **19**, **20** are the prior experiments showing that in the presence of VTMS **10c**, **11c** are in equilibrium with bis-vinyl TMS complexes **4**, **5** (via return through **19**, **20**) prior to ketone formation.

Reactions between excess PMe_3 and **15c** or **16c** at 50 °C were performed to study the reductive elimination of ketone. Rate constants for the reductive elimination of ketone from **15/16** and trapping with PMe_3 to form **17/18** were measured by ^1H NMR spectroscopy at 50 °C by simply heating the reaction mixtures that resulted from the kinetic studies of the CO insertion step. Data is summarized in Table 5, column 6. Clean first-order kinetics were observed with measured rate constants of 2.0×10^{-5} and $2.6 \times 10^{-5} \text{ s}^{-1}$ for the reductive elimination of ketone from **16c** with 5 and 10 equiv PMe_3 , respectively. The lack of dependence of the rate of reductive elimination on $[\text{PMe}_3]$ suggests that C–C bond formation is the rate-determining step of the reductive elimination, followed by rapid loss of ketone and formation of bis- PMe_3 complex **18**.

(55) Luo, X.; Tang, D.; Li, M. *THEOCHEM* 2005, 730, 177–183.

Scheme 5



Scheme 6

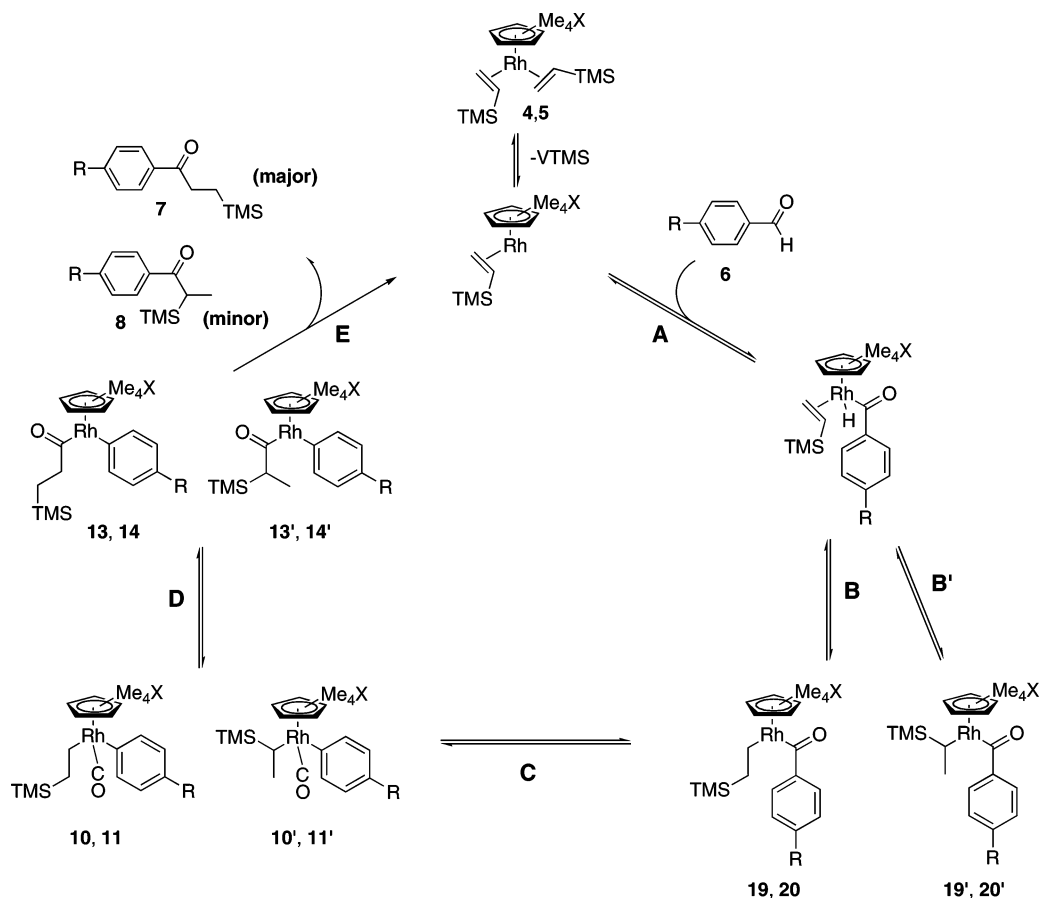


Table 5. Rate Constants for CO Insertion and Reductive Elimination Steps

compound	X	R	[PMe ₃] (M)	<i>k</i> ₁ (× 10 ⁴ s ⁻¹), 25 °C	<i>k</i> _{RE} (× 10 ⁵ s ⁻¹), 50 °C
15a	CH ₃	NMe ₂	0.18	N/A	0.33
			0.36	N/A	0.33
16a	CF ₃	NMe ₂	0.18	N/A	fast at 25 °C
			0.36	N/A	fast at 25 °C
10c/15c	CH ₃	CH ₃	0.18	0.83	very slow at 50 °C
			0.36	1.5	very slow at 50 °C
11c/16c	CF ₃	CH ₃	0.18	0.50	2.0
			0.36	1.1	2.6

Accurate rate constants for the reductive elimination of ketone from **15c** could not be measured due to negligible formation of ketone from **15c** at 50 °C. Instead, the rate of reductive elimination of ketone from **15a**, with a dimethylamino substituent on the aryl group, was measured. Rate constants of $0.33 \times 10^{-5} \text{ s}^{-1}$ were measured for reactions of **15a** with 5 and 10 equiv of PMe₃. A direct comparison to the rate of reductive

elimination from the analogous complex with the Cp⁺ ligand (**16a**) could not be made because **16a** underwent reductive elimination of ketone at room temperature, and thus **16a** could not be cleanly isolated for subsequent studies. However, the fact that **16a** underwent reductive elimination at room temperature, whereas **15a** did not, indicates that **16a** should have a significantly lower barrier for reductive elimination than **15a**. This conclusion is supported by the observation that **16c** underwent reductive elimination at a measurable rate at 50 °C, while **15c** did not. Thus, the substitution of one CF₃ group for a CH₃ group of the cyclopentadienyl ligand significantly increases the rate of reductive elimination of ketone, as expected based on a more electron-deficient rhodium center in the case of the CF₃-substituted system.

G. Summary of the Proposed Catalytic Cycle for Rh-Catalyzed Hydroacylation of Olefins by Aryl Aldehydes. The results described above are consistent with the mechanism illustrated in Scheme 6 for hydroacylation of vinyltrimethylsilane. Initial dissociation of olefin forms a 16-electron intermedi-

ate that rapidly binds aldehyde to form a reactive Rh aldehyde olefin complex. Oxidative addition of the aldehyde C–H bond is fast and reversible to form a Rh(III) acyl hydride intermediate (step A). Olefin insertion can then occur with either regiochemistry to generate a linear (step B) or branched (step B') alkyl-acyl Rh intermediate. In the case of the Cp*-based system, steps A and B, B' must be reversible to account for loss of deuterium from deuterated aldehyde and for the pattern of deuterium labeling in the Rh(III) alkyl aryl carbonyl complex **10**. For the Cp[†]-based system, formation of the linear isomer **11** (via **20**) is fast and reversible, but the D labeling pattern suggests that the barrier for formation of the branched isomer, **20'**, is substantially higher and that product formation occurs with a lower barrier than formation of **11'**, leading to high selectivity for the linear ketone.

The deinsertion of CO in step C generates Rh(III) complexes **10/11**, one of the dual resting states observed during the reaction. Steps A, B, and C, leading to the formation of **10/11**, must all be reversible to explain the results of the aldehyde exchange experiments. CO insertion then occurs reversibly in step D to generate the rhodium acyl aryl intermediate that then reductively eliminates ketone in the turnover-limiting step of the reaction. The increased activity of catalyst **5**, relative to **4**, for the hydroacylation of olefins is attributed to an increase in the rate of reductive elimination for complexes with the more electron-withdrawing Cp[†] ligand. While only very minor amounts of branched Cp*[†]Rh(CH₂CH₂SiMe₃)(aryl)(CO) complex **10'** are present, a significant fraction of the ketone product (ca 33%) is branched, suggesting that reductive elimination from the branched Cp*[†]Rh(alkyl)(aryl)(CO) isomer **10'** (which is in equilibrium with the linear isomer, **10**) occurs considerably faster than reductive elimination from the linear isomer.

Several additional points should be made concerning this scheme: (1) Product ketones could form from the reductive elimination from the alkyl aryoyl complexes.^{19,20} However, such reductive elimination would require C(sp³)–C(sp²) coupling which should be less favorable than C(sp²)–C(sp²) coupling required for product formation from **13,14**. Thus, we favor product formation from **13,14**. (2) The structures of the Rh(III) acyl and aryoyl complexes **13,14** and **19,20** are depicted as 16-electron species. However, they may well exist as 18-electron η² acyl complexes. We do not have experimental data to distinguish these possibilities. (3) In addition to the fact that the turnover frequency is greater for the more electron-deficient Cp[†]-based system, the achievable turnover numbers are also higher for the Cp[†] systems. This implies that the catalyst decay rate relative to the turnover frequency must be greater for the Cp* system. Catalyst decay occurs via decarbonylation and formation of arene. Decarbonylation must involve reductive elimination of aryl hydride from a Rh(I) center. However, the mechanistic details of this decarbonylation process and the rate-limiting step are not known, thus it is unclear why product formation, relative to decarbonylation, is more favored in the case of Cp[†] catalysts. (4) Despite the fact that between the equilibrating resting states (**4/5** with **10/11**) the Rh(III) alkyl aryl carbonyl species (**10,11**) are more populated for the electron-deficient aldehydes, these aldehydes yield fewer total turnovers. This must arise from some combination of more rapid decarbonylation (catalyst death) and more sluggish reductive elimination due to a stronger Rh–aryl bond. (5) It is likely a

similar catalytic cycle applies to reactions of other olefins in Table 2. However, the relative rates of interconversion of species and the relative stabilities of the resting states will surely change with the nature of the olefin. It is interesting to note that a similar trend for regioselectivity in product formation is observed in the case of 1-hexene. The Cp[†]-derived catalyst **5** yields highly linear product (22:1, linear:branched), whereas the Cp*-based catalyst **4** is unselective (3:2 linear:branched ketone).

Experimental Section

General Considerations. All manipulations were carried out using standard Schlenk and glovebox techniques. Argon was purified by passage through columns of BASF R3–11 (Chemalog) and 4 Å molecular sieves. All solvents used for synthesis, except tetrahydrofuran, were deoxygenated and dried via passage over a column of activated alumina.⁵⁶ Tetrahydrofuran was distilled from sodium benzophenone ketyl prior to use. NMR spectra were recorded on Bruker DRX 400 and AMX 300 MHz instruments and are referenced to residual protio solvent. ³¹P NMR chemical shifts are referenced to an external 85% H₃PO₄ standard. GC analysis was performed on an Agilent 6850 Series GC with a dimethylpolysiloxane column (Agilent HP-1). Elemental analyses were performed by Atlantic Microlabs, Inc., of Norcross, GA. [C₅Me₅Rh(C₂H₃SiMe₃)₂], (1,2,3,4)-Me₄-5-CF₃-cyclopentadiene (Cp[†]H), [Cp[†]RhCl₂]₂, and 4-(dimethylamino)benzaldehyde-*d*₁ were prepared following reported procedures.^{47,53,57} All aldehydes and olefins listed were purchased from Aldrich. Aldehydes were purified via recrystallization or distillation before use, and olefins were dried and distilled prior to use. Benzene-*d*₆ and toluene-*d*₈ were dried over potassium benzophenone ketyl, vacuum transferred, and degassed. Acetone-*d*₆ and acetophenone-*d*₈ were dried over CaH₂, vacuum transferred and degassed.

Synthesis of Cp[†]Rh(H₂C=CH–SiMe₃)₂ (5**).** Under an argon atmosphere, 995 mg (1.37 mmol) of [Cp[†]RhCl₂]₂ and 1.82 g (27.8 mmol) of Zn powder were weighed into an oven-dried Schlenk flask. THF (25 mL) was added to the flask via syringe, followed by 4.0 mL (27 mmol) of vinyltrimethylsilane. The red suspension was stirred vigorously overnight. The resulting brown suspension was filtered through celite to remove insoluble zinc species, and THF was evaporated under vacuum. The product was extracted the pentane, and the pentane was evaporated under vacuum to yield 1.10 g (81% yield) of the clean, yellow/orange solid. This solid can also be recrystallized from acetone at –78 °C. ¹H NMR (CD₂Cl₂): δ 0.082 (s, 18H), 1.35 (br s, 1H), 1.38 (br s, 1H), 1.48–1.50 (br m, 1H), 1.51–1.53 (br m, 1H), 1.56–1.57 (3H), 1.71 (s, 3H), 1.74–1.75 (br, 3H), 2.03 (s, 3H), 2.54 (dd, *J* = 11.2 Hz, 2.4 Hz, 2H). ¹³C NMR (acetone-*d*₆): δ 2.17, 7.91 (br q, *J* = 1.4 Hz), 8.61, 9.93 (br q, *J* = 1.6 Hz), 10.95, 49.13 (d, *J* = 13.6 Hz), 49.56 (d, *J* = 13.8 Hz), 90.49 (q of d, *J* = 31.3 Hz, 6.1 Hz), 96.10, 98.20, 102.04, 104.25, 126.80 (q, *J* = 269.1 Hz). Anal. Calcd for C₂₀H₃₆F₃Si₂Rh: C, 48.76; H, 7.38. Found: C, 49.07; H, 7.63.

General Procedure for the Synthesis of Intermediates **10, 11.** In the drybox, rhodium bis-olefin complex **4** or **5** was weighed into a flame-dried Kontes flask. The flask was removed from the box and purged with argon on the Schlenk line. Anhydrous toluene (10 mL) was added, along with 1.1 equiv of the desired aldehyde. The reaction mixture was stirred at room temperature and was monitored periodically by TLC and/or ¹H NMR spectroscopy. Once the reaction was finished, the volatiles were removed under vacuum and the residue dried under vacuum overnight. Attempts to purify the products by recrystallization

- (56) Pangborn, A. B.; Giardello, M. A.; Grubbs, R. H.; Rosen, R. K.; Timmers, F. J. *Organometallics* **1996**, *15*, 1518–1520.
 (57) Barletta, G. L.; Zou, Y.; Huskey, W. P.; Jordan, F. J. *Am. Chem. Soc.* **1997**, *119*, 2356–2362.
 (58) Akhrem, I. S.; Churilova, I. M.; Orlinkov, A. V.; Afanas'eva, L. V.; Vitt, S. V.; Petrovskii, P. V. *Russ. Chem. Bull.* **1998**, *47* (5), 918–923.
 (59) Faussett, B. W.; Liebeskind, L. S. *J. Org. Chem.* **2005**, *70* (12), 4851–4853.

or by chromatography failed, so the product was characterized by ^1H and ^{13}C NMR and by IR spectroscopy with small amounts of residual starting materials or ketone (from reductive elimination) present.

$\text{Cp}^*\text{Rh}(\text{CH}_2\text{CH}_2\text{SiMe}_3)(\text{CO})(4\text{-NMe}_2\text{-C}_6\text{H}_4)$ (10a). $\text{Cp}^*\text{Rh}(\text{VTMS})_2$ (84 mg, 0.19 mmol) and 4-(dimethylamino)benzaldehyde (31 mg, 0.21 mmol) were employed to prepare **10a**. ^1H NMR (C_6D_6): δ 0.064 (s, SiMe_3), 1.73 (dt, $J = 13.6, 4.4$ Hz, 1H), 1.17–1.22 (m, 1H), 1.51 (s, 15H), 1.75–1.86 (m, 1H), 1.90–2.10 (m, 1H), 2.63 (s, 6H), 6.68 (d, $J = 8.8$ Hz, 2H), 7.16 (d, 8.0 Hz, 2H).

$\text{Cp}^*\text{Rh}(\text{CH}_2\text{CH}_2\text{SiMe}_3)(\text{CO})(4\text{-OMe-C}_6\text{H}_4)$ (10b). $\text{Cp}^*\text{Rh}(\text{VTMS})_2$ (79 mg, 0.18 mmol) and 4-methoxybenzaldehyde (24 μL , 0.20 mmol) were employed to prepare **10b**. ^1H NMR (C_6D_6): δ 0.054 (s, 9H), 1.05 (dt, $J = 14.0$ Hz, 4.4 Hz, 1H), 1.17 (dt, $J = 13.6$ Hz, 4.4 Hz, 1H), 1.48 (s, 15H), 1.76–1.84 (m, 1H), 1.92–1.99 (m, 1H), 3.43 (s, 3H), 6.83 (d, $J = 6.8$ Hz, 2H), 7.17 (d, $J = 7.2$ Hz, 2H). ^{13}C NMR (C_6D_6): δ -1.78 (s, SiMe_3), 9.08 (s, C_5Me_5), 18.00 (d, $J = 24.1$ Hz, $\text{Rh-C}_{\text{alkyl}}$), 54.62 (s, OMe), 101.99 (s, C_5Me_5), 114.84 (s), 139.05 (s), 141.40 (d, $J = 36.2$ Hz, $\text{Rh-C}_{\text{aryl}}$), 157.61 (s), 194.62 (d, $J = 81.7$ Hz, CO). IR: 1994 cm^{-1} .

$\text{Cp}^*\text{Rh}(\text{CH}_2\text{CH}_2\text{SiMe}_3)(\text{CO})(4\text{-CH}_3\text{-C}_6\text{H}_4)$ (10c). $\text{Cp}^*\text{Rh}(\text{VTMS})_2$ (79 mg, 0.18 mmol) and 4-tolualdehyde (24.5 μL , 0.20 mmol) were employed to prepare **10c**. ^1H NMR (C_6D_6): δ 0.057 (s, 9H), 1.06 (dt, $J = 14.4$ Hz, 4.0 Hz, 1H), 1.18 (dt, $J = 13.6$ Hz, 4.4 Hz, 1H), 1.48 (s, 15H), 1.78–1.87 (m, 1H), 1.93–2.10 (m, 1H), 2.23 (s, 3H), 6.99 (d, $J = 7.6$ Hz, 2H), 7.24 (d, $J = 6.4$ Hz, 2H). ^{13}C NMR (C_6D_6): δ -1.78 (s, SiMe_3), 9.08 (s, C_5Me_5), 18.05 (d, $J = 24.2$ Hz, $\text{Rh-C}_{\text{alkyl}}$), 20.97 (s, tolyl CH_3), 26.03 (s), 101.97 (s, C_5Me_5), 129.35 (s), 132.14 (s), 138.95 (s), 149.44 (d, $J = 35.6$ Hz, $\text{Rh-C}_{\text{aryl}}$), 194.61 (d, $J = 81.8$ Hz, CO). IR: 1995 cm^{-1} .

$\text{Cp}^*\text{Rh}(\text{CH}_2\text{CH}_2\text{SiMe}_3)(\text{CO})(\text{C}_6\text{H}_5)$ (10d). $\text{Cp}^*\text{Rh}(\text{VTMS})_2$ (78 mg, 0.18 mmol) and benzaldehyde (20 μL , 0.20 mmol) were employed to prepare **10d**. ^1H NMR (C_6D_6): δ 0.047 (s, 9H), 1.05 (dt, $J = 14.4$ Hz, 4.0 Hz, 1H), 1.17 (dt, $J = 13.6$ Hz, 4.8 Hz, 1H), 1.45 (s, 15H), 1.78–1.86 (m, 1H), 1.92–2.10 (m, 1H), 7.05 (t, $J = 6.8$ Hz, 1H), 7.13 (t, $J = 7.6$ Hz, 2H), 7.33 (d, $J = 7.2$ Hz, 2H). ^{13}C NMR (C_6D_6): δ -1.78 (s, SiMe_3), 9.04 (s, C_5Me_5), 18.12 (d, $J = 23.9$ Hz, $\text{Rh-C}_{\text{alkyl}}$), 26.09 (s), 102.00 (s, C_5Me_5), 123.49 (s), 128.36 (s), 139.25 (s), 154.35 (d, $J = 35.5$ Hz, $\text{Rh-C}_{\text{aryl}}$), 194.53 (d, $J = 81.9$ Hz, CO). IR: 1998 cm^{-1} .

$\text{Cp}^*\text{Rh}(\text{CH}_2\text{CH}_2\text{SiMe}_3)(\text{CO})(4\text{-CF}_3\text{-C}_6\text{H}_4)$ (10e). $\text{Cp}^*\text{Rh}(\text{VTMS})_2$ (102 mg, 0.23 mmol) and 4-trifluoromethylbenzaldehyde (34 μL , 0.25 mmol) were employed to prepare **10e**. ^1H NMR (C_6D_6): δ 0.040 (s, 9H), 1.01 (dt, $J = 14.0$ Hz, 4.7 Hz, 1H), 1.09 (dt, $J = 14.0$ Hz, 4.8 Hz, 1H), 1.35 (s, 15H), 1.77 (m, 1H), 1.86 (m, 1H), 7.31 (m, 4H). ^{13}C NMR (C_6D_6): δ -1.87 (s, SiMe_3), 8.86 (s, C_5Me_5), 18.50 (d, $J = 23$ Hz, $\text{Rh-C}_{\text{alkyl}}$), 26.20 (s), 102.16 (s, C_5Me_5), 123.95 (q, $J = 2.0$ Hz), 125.89 (q, $J = 32$ Hz, $\text{C}_{\text{aryl}}\text{-CF}_3$), 126.13 (q, $J = 271$ Hz, CF_3), 139.56 (s), 162.8 (d, $J = 37$ Hz, $\text{Rh-C}_{\text{aryl}}$), 194.0 (d, $J = 81$ Hz, CO). IR: 2000 cm^{-1} .

$\text{Cp}^*\text{Rh}(\text{CH}_2\text{CH}_2\text{SiMe}_3)(\text{CO})(4\text{-NMe}_2\text{-C}_6\text{H}_4)$ (11a). $\text{Cp}^*\text{Rh}(\text{VTMS})_2$ (8.3 mg, 0.017 mmol) and 4-(dimethylamino)benzaldehyde (24 mg, 0.16 mmol) were employed to prepare **11a** in situ. ^1H NMR (C_6D_6): δ 0.037 (s, 9H), 1.15 (m, 2H), 1.21 (s, 3H), 1.28 (s, 3H), 1.68 (s, 3H), 1.78 (s, 3H), 2.15 (m, 2H), 2.58 (s, 6H), 6.66 (d, $J = 8.8$ Hz, 2H), 7.13 (d, 2H; half of doublet overlaps with residual solvent peak, so no J value calculated).

$\text{Cp}^*\text{Rh}(\text{CH}_2\text{CH}_2\text{SiMe}_3)(\text{CO})(4\text{-Me-C}_6\text{H}_4)$ (11c). $\text{Cp}^*\text{Rh}(\text{VTMS})_2$ (100 mg, 0.20 mmol) and 4-tolualdehyde (28 μL , 0.23 mmol) were employed to prepare **11c**. ^1H NMR (C_6D_6): δ 0.055 (s, 9H), 1.12–1.22 (m, 2H, CH_2), 1.21 (s, 3H), 1.29 (s, 3H), 1.68 (s, 3H), 1.80 (s, 3H), 2.10–2.16 (m, 2H, CH_2), 2.23 (s, 3H), 6.97 (d, $J = 7.6$ Hz, 2H), 7.19 (d, $J = 8.0$ Hz, 2H). ^{13}C NMR (C_6D_6): δ -1.89 (s, SiMe_3), 8.17 (s), 9.47 (s), 9.93 (s), 10.49 (s), 20.20 (d, $J = 23.3$ Hz, $\text{Rh-C}_{\text{alkyl}}$), 26.27 (s), 91.52 (q, $J = 34.5$ Hz, C-CF_3), 102.94 (s), 103.46 (s), 106.73 (s), 109.15 (s), 125.71 (q, $J = 270.5$ Hz, CF_3), 129.79 (s), 132.99 (s), 138.47 (s), 145.55 (d, $J = 34.7$ Hz, $\text{Rh-C}_{\text{aryl}}$), 192.36 (d, $J = 82.2$ Hz, CO).

$\text{Cp}^*\text{Rh}(\text{CH}_2\text{CH}_2\text{SiMe}_3)(\text{CO})(\text{C}_6\text{H}_5)$ (11d). $\text{Cp}^*\text{Rh}(\text{VTMS})_2$ (81 mg, 0.17 mmol) and benzaldehyde (19 μL , 0.19 mmol) were employed to prepare **11d**. ^1H NMR (C_6D_6): δ -0.001 (s, 9H), 1.04–1.17 (m, 2H), 1.14 (s, 3H), 1.22 (s, 3H), 1.60 (s, 3H), 1.74 (s, 3H), 2.05–2.11 (m, 2H), 7.01 (t, $J = 7.2$ Hz, 1H), 7.06 (t, $J = 7.6$ Hz, 2H), 7.23 (d, $J = 7.2$ Hz, 2H). ^{13}C NMR (C_6D_6): δ -1.89 (s, SiMe_3), 8.14 (s), 9.43 (s), 9.88 (s), 10.48 (s), 20.31 (d, $J = 23.2$ Hz, $\text{Rh-C}_{\text{alkyl}}$), 26.32 (s), 91.60 (q, $J = 33.9$ Hz, C-CF_3), 102.66 (s), 103.47 (s), 106.77 (s), 109.18 (s), 124.13 (s), 125.67 (q, $J = 270.6$ Hz, CF_3), 128.75 (s), 138.77 (s), 150.30 (d, $J = 34.6$ Hz, $\text{Rh-C}_{\text{aryl}}$), 192.25 (d, $J = 83.9$ Hz, CO). IR: 2016 cm^{-1} .

Synthesis of $\text{Cp}^*\text{Rh}(\text{C}(\text{O})\text{CH}_2\text{CH}_2\text{SiMe}_3)(\text{PMe}_3)(\text{Ph})$ (15d). Into a flame-dried Schlenk flask was weighed $\text{Cp}^*\text{Rh}(\text{VTMS})_2$ (292.0 mg, 0.666 mmol). Anhydrous toluene (8 mL) and freshly distilled benzaldehyde (84 μL , 0.821 mmol) were added via syringe, and the mixture was stirred under argon at room temperature for about a week. Volatiles were evaporated under vacuum to leave brown oil. PMe_3 (0.65 mL, 6.28 mmol) and 5 mL of toluene were added, and the mixture was stirred at room temperature overnight. Volatiles were evaporated and the resulting brown oil was dried under vacuum. ^1H NMR (C_6D_6): δ 0.071 (s, 9H), 1.03 (d, $J = 11.6$ Hz, 9H), 1.18 (m, 1H), 1.31 (qd, $J = 5.2, 12.0, 15.2$ Hz, 1H), 1.61 (d, $J = 2.0$ Hz, 15H), 2.69 (qd, $J = 4.8, 11.6, 16.8$ Hz, 1H), 3.43 (qd, $J = 4.4, 11.6, 16.4$ Hz, 1H), 6.98 (t, $J = 6.8$ Hz, 1H), 7.06 (t, $J = 7.2$ Hz, 2H), 7.25 (d, $J = 8.0$ Hz, 2H). ^{13}C NMR (C_6D_6): δ -1.69 (s, SiMe_3), 10.37 (s, C_5Me_5), 13.47 (s, CH_2), 14.85 (d, $J = 32.9$ Hz, PMe_3), 51.75 (s, CH_2), 100.50 (t, $J = 9.2$ Hz, C_5Me_5), 121.76 (s), 126.71 (s), 140.84 (s), 156.5 (dd, $J_{\text{Rh-C}}, J_{\text{P-C}} = 20.3, 18.5$ Hz), 199.30 (d, $J = 63.6$ Hz, CO).

General Procedure for the Reaction of Aromatic Aldehydes with Olefins. The reaction conditions and average yields for each reaction are shown in Table 2. A typical procedure is given for the first entry in Table 2.

4-NMe₂-C₆H₄-C(O)CH₂CH₂SiMe₃.⁴⁰ Into a thick-walled 4 mL flask were weighed 123 mg (0.821 mmol) of 4-(dimethylamino)benzaldehyde and 20.2 mg (0.0410 mmol) of $\text{Cp}^*\text{Rh}(\text{VTMS})_2$. Subsequently, 1.2 mL (8.2 mmol) of vinyltrimethylsilane and 1.2 mL of toluene were added to the flask via syringe. The flask was sealed with a Kontes Teflon screw cap and placed in a 100 °C bath. The solution was stirred at 100 °C until the aldehyde was completely consumed, as determined by GC. After evaporation of the solvent, the residue was purified by chromatography on silica gel (100% hexanes to elute small brown band, then hexanes:ethyl acetate = 9:1 to elute colorless product) to yield 164 mg (80% yield) of 4-NMe₂-C₆H₄-C(O)CH₂CH₂SiMe₃ as a white solid. ^1H NMR (CDCl_3): δ 0.030 (s, 9H), 0.85–0.90 (m, 2H), 2.80–2.85 (m, 2H), 3.04 (s, 6H), 6.69 (d, $J = 9.2$ Hz, 2H), 7.86 (d, $J = 9.2$ Hz, 2H). ^{13}C NMR (CD_2Cl_2): δ -1.66 (3C), 11.70, 32.57, 40.18 (2C), 110.96 (2C), 125.05, 130.36 (2C), 153.64, 199.33.

4-NMe₂-C₆H₄-C(O)(C₅H₉). 4-NMe₂-C₆H₄CHO (100 mg, 0.674 mmol), cyclopentene (0.60 mL, 6.79 mmol), $\text{Cp}^*\text{Rh}(\text{VTMS})_2$ (16.6 mg, 0.0337 mmol), and 0.6 mL of toluene was used, and the solution was stirred at 75 °C. The crude product was purified by chromatography on silica gel (100% hexanes to elute small brown band, then hexanes:ethyl acetate = 9:1 to elute colorless product) to give 139 mg (95% yield) of 4-NMe₂-C₆H₄-C(O)C₅H₉ as a white solid. ^1H NMR (CD_2Cl_2): δ 1.62–1.69 (m, 4H), 1.81–1.88 (m, 4H), 3.04 (s, 6H), 3.64 (quintet, $J = 7.6$ Hz, 1H), 6.67 (d, $J = 7.2$ Hz, 2H), 7.86 (d, $J = 6.8$ Hz, 2H). ^{13}C NMR (CD_2Cl_2): δ 26.71 (2C), 30.55 (2C), 40.17 (2C), 45.90, 110.95 (2C), 125.17, 130.69 (2C), 153.61, 200.78. Anal. Calcd for $\text{C}_{14}\text{H}_{19}\text{NO}$: C, 77.36; H, 8.83; N, 6.45. Found: C, 77.12; H, 8.86; N, 6.50.

4-MeO-C₆H₄-C(O)(C₅H₉).⁵⁸ 4-MeO-C₆H₄CHO (80 μL , 0.658 mmol), cyclopentene (0.60 mL, 6.79 mmol), $\text{Cp}^*\text{Rh}(\text{VTMS})_2$ (22.7 mg, 0.0461 mmol), and 0.6 mL toluene were used, and the solution was stirred at 75 °C. The crude product was purified by chromatography on silica gel (100% hexanes to elute small brown band, then hexanes:ethyl acetate = 9:1 to elute colorless product) to give 124 mg (93%

yield) of 4-MeO-C₆H₄-C(O)(C₅H₉) as a white solid. ¹H NMR (CD₂-Cl₂): δ 1.63–1.72 (m, 4H), 1.83–1.91 (m, 4H), 3.67 (quintet, *J* = 8.4 Hz, 1H), 3.86 (s, 3H), 6.95 (d, *J* = 7.2 Hz, 2H), 7.95 (d, *J* = 7.2 Hz, 2H). ¹³C NMR (CD₂Cl₂): δ 26.66 (2C), 30.38 (2C), 46.36, 55.82, 113.94 (2C), 130.37, 130.89 (2C), 163.58, 201.36.

4-Me-C₆H₄-C(O)(C₅H₉).^{58, 59} 4-Me-C₆H₄CHO (78 μL, 0.662 mmol), cyclopentene (0.60 mL, 6.79 mmol), Cp⁺Rh(VTMS)₂ (22.8 mg, 0.0463 mmol), and 0.6 mL toluene were used, and the solution was stirred at 75 °C. The crude product was purified by chromatography on silica gel (100% hexanes to elute small brown band, then hexanes: ethyl acetate = 9:1 to elute colorless product) to give 101 mg (81% yield) of 4-Me-C₆H₄-C(O)(C₅H₉) as a white solid. ¹H NMR (CD₂-Cl₂): δ 1.62–1.72 (m, 4H), 1.82–1.94 (m, 4H), 2.40 (s, 3H), 3.69 (quintet, *J* = 7.2 Hz, 1H), 7.26 (d, *J* = 8.0 Hz, 2H), 7.84 (d, *J* = 8.0 Hz, 2H). ¹³C NMR (CD₂Cl₂): δ 21.65, 26.65 (2C), 30.31 (2C), 46.60, 128.80 (2C), 129.51 (2C), 134.78, 143.84, 204.84.

4-NMe₂-C₆H₄-C(O)(C₇H₁₁). 4-NMe₂-C₆H₄CHO (124 mg, 0.828 mmol), norbornene (762 mg, 8.09 mmol), Cp⁺Rh(VTMS)₂ (20.4 mg, 0.0414 mmol), and 1.2 mL toluene were used, and the solution was stirred at 75 °C. The crude product was purified by chromatography on silica gel (100% hexanes to elute small brown band, then hexanes: ethyl acetate = 9:1 to elute colorless product) to give 192 mg (95% yield) of 4-NMe₂-C₆H₄-C(O)(C₇H₁₁) as a white solid. ¹H NMR (CD₂-Cl₂): δ 1.10–1.13 (m, 1H), 1.29–1.31 (m, 1H), 1.36–1.47 (m, 3H), 1.55–1.60 (m, 2H), 1.92–1.99 (m, 1H), 2.29 (br, 1H), 2.43 (br, 1H), 3.04 (s, 6H), 3.14 (dd, *J* = 5.6, 8.8 Hz, 1H), 6.67 (d, *J* = 9.2 Hz, 2H), 7.85 (d, *J* = 9.2 Hz, 2H). ¹³C NMR (CD₂Cl₂): δ 29.41, 30.04, 34.08, 36.49, 36.69, 40.16, 41.72, 48.96, 110.92, 124.77, 130.66, 153.51, 199.50. Anal. Calcd for C₁₆H₂₁NO: C, 78.95; H, 8.71; N, 5.76. Found: C, 78.65; H, 8.71; N, 5.81.

4-NMe₂-C₆H₄-C(O)CH₂CH₂C(CH₃)₃. 4-NMe₂-C₆H₄CHO (123 mg, 0.822 mmol), 3,3-dimethyl-1-butene (0.94 mL, 7.29 mmol), Cp⁺-Rh(VTMS)₂ (20.2 mg, 0.0411 mmol), and 1.0 mL toluene were used, and the solution was stirred at 75 °C. The crude product was purified by chromatography on silica gel (100% hexanes to elute small brown band, then hexanes:ethyl acetate = 9:1 to elute colorless product) to give 188 mg (98% yield) of 4-NMe₂-C₆H₄-C(O)CH₂CH₂C(CH₃)₃ as a white solid. ¹H NMR (CD₂Cl₂): δ 0.95 (s, 9H), 1.55–1.60 (m, 2H), 2.79–2.84 (m, 2H), 3.04 (s, 6H), 6.67 (d, *J* = 6.8 Hz, 2H), 7.84 (d, *J* = 7.2 Hz, 2H). ¹³C NMR (CD₂Cl₂): δ 29.35 (3C), 30.46, 33.87, 39.10, 40.19 (2C), 110.94 (2C), 125.38, 130.37 (2C), 153.70, 199.11. Anal. Calcd for C₁₅H₂₃NO: C, 77.19; H, 9.95; N, 6.00. Found: C, 76.75; H, 9.93; N, 6.02.

4-NMe₂-C₆H₄-C(O)CH₂CH₂CH₂CH₂CH₂CH₃. 4-NMe₂-C₆H₄-CHO (124 mg, 0.832 mmol), 1-hexene (1.2 mL, 9.6 mmol), Cp⁺Rh-(VTMS)₂ (20.5 mg, 0.0416 mmol), and 1.2 mL toluene were used, and the solution was stirred at 100 °C. The crude product was purified by chromatography on silica gel (100% hexanes to elute small brown band, then hexanes:ethyl acetate = 9:1 to elute colorless product) to give 173 mg (89% yield) of 4-NMe₂-C₆H₄-C(O)CH₂CH₂CH₂CH₂CH₂CH₃ as a white solid. ¹H NMR (CD₂Cl₂): δ 0.89 (m, 3H), 1.26–1.40 (m, 6H), 1.67 (quintet, *J* = 7.6 Hz, 2H), 2.86 (t, *J* = 7.6 Hz, 2H), 3.04 (s, 6H), 6.66 (d, *J* = 9.2 Hz, 2H), 7.84 (d, *J* = 8.8 Hz, 2H). ¹³C NMR (CD₂Cl₂): δ 14.25, 23.00, 25.31, 29.59, 32.17, 38.23, 40.21, 110.95 (2C), 125.50, 130.37 (2C), 153.71, 198.69. Anal. Calcd for C₁₅H₂₃NO: C, 77.19; H, 9.95; N, 6.00. Found: C, 76.90; H, 9.98; N, 6.06.

Representative Procedure for Measurement of Rate Constants for Reaction of 10/11 with PMe₃ to form 15/16. Complex **5** (9.8 mg, 0.020 mmol) was dissolved in 0.5 mL C₆D₆ in a J Young tube. *p*-Tolualdehyde (30 μL, 0.25 mmol) and 1,3,5-trimethoxybenzene (100 μL of a 0.1 M stock solution in C₆D₆) were added, and the contents were allowed to react at room temperature. The reaction was monitored by ¹H NMR spectroscopy. Upon full conversion to **11c**, PMe₃ (21 μL, 0.20 mmol) was added to the mixture, and the reaction was performed at 25 °C in the probe of a 500 MHz NMR spectrometer. ¹H NMR spectra were obtained at regular time intervals until **11c** was fully converted to **16c**.

Representative Procedure for Measurement of Rate Constants for Reductive Elimination of Ketone from 15/16. The J Young tube containing the reaction mixture from the formation of **16c** (above) was heated to 50 °C in the probe of a 500 MHz NMR spectrometer, and ¹H NMR spectra were obtained at regular time intervals over 3–5 half-lives.

Acknowledgment. We gratefully acknowledge funding by the National Institutes of Health (Grant No. GM 28938).

Supporting Information Available: CIF file containing X-ray crystallographic data for complex **15d**, and figures showing kinetic plots for the conversion of **5** to **11c** and for the reductive elimination of ketone from **16c**. This material is available free of charge via the Internet at <http://pubs.acs.org>.

JA066509X